The Synergy between Deep X-ray and Infrared Surveys: AGN and Star Formation Activity

J. R. Mullaney and D. M. Alexander

University of Durham, U. K.

Abstract. We explore the connections between the infrared and X-ray properties of AGNs. Using the well constrained infrared SEDs of a sample of local (i.e., $z < 0.1$) sample of X-ray AGNs, we develop new diagnostics that exploit 24 μm and 70 μm flux densities to identify AGN-dominated systems at $z < 1.5$ and measure their total infrared luminosities. We apply these diagnostics to the X-ray detected AGNs in the Chandra Deep Field South and, in doing so, reveal that the infrared to X-ray luminosity ratio was a factor of ~ 12 higher in the early Universe compared to today. We explore possible explanations for this dramatic evolution and demonstrate how forthcoming *Herschel* observations will discriminate between these scenarios and, while doing so, identify potential Compton-thick AGNs. Summary of Mullaney et al. [1].

Keywords: Far-Infrared, Active Galactic Nuclei
PACS: 98

INTRODUCTION

With their ability to penetrate large columns of gas and dust, observations at both X-ray and infrared wavelengths are complementary in the study of active galactic nuclei (hereafter, AGNs). While X-rays provide a largely uncontaminated view of the primary emission process, measures of infrared emission yield detailed information about the levels of dust and on-going star-formation surrounding AGNs. Consequently, by combining results from both X-ray and infrared observations, we can address some of the key remaining questions concerning AGNs and their to links galaxy evolution, such as (1) the properties of the obscuring AGN dusty torus and how it has evolved with time, (2) the relative ratio between galaxy and black hole growth (i.e., star-formation and AGN activity) over cosmic time and (3) the numbers of X-ray weak, infrared bright Compton-thick AGNs in the Universe.

Here, we provide a summary of our recently published investigation into the mid to far-infrared (MIR [5-30 μm] and FIR [30-300 μm], respectively) properties of X-ray detected AGNs out to $z \sim 2$ (see Mullaney et al. [1]). As part of this study, we develop new MIR/FIR diagnostics to identify those systems dominated by AGN activity and derive their total infrared output (across 8-1000 μm; hereafter, $L_{\rm IR}$) from their 24 μm and 70 μm flux densities (hereafter, S_{24} and S_{70}, respectively). We then use these diagnostics to explore how the infrared properties of X-ray detected AGNs vary as a function of redshift and intrinsic power (assumed to correlate with X-ray luminosity, $L_{\rm X}$). In doing so, we find that the average infrared to X-ray luminosity ratio ($L_{\rm IR}/L_{\rm X}$) of moderate luminosity AGNs has evolved strongly over cosmic time. Finally, we explore how these diagnostics will be combined with the results from planned *Herschel* surveys

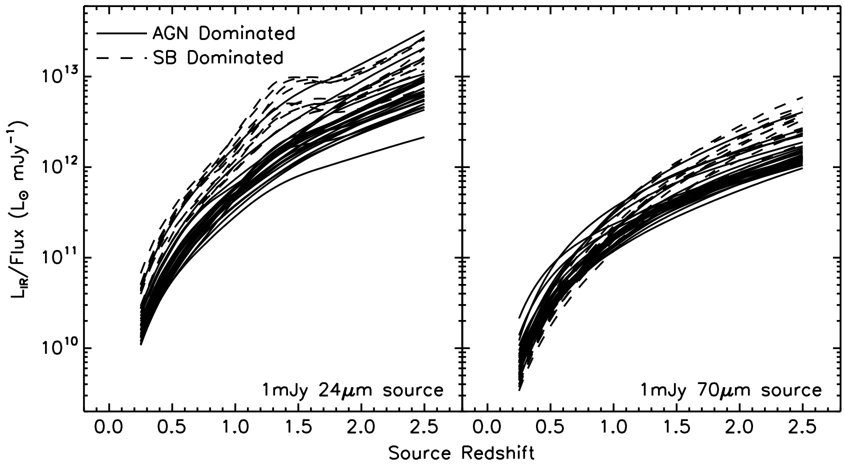

FIGURE 1. $L_{\rm IR}/S_{24}$ and $L_{\rm IR}/S_{70}$ ratios derived from our local sample of AGNs as a function of redshift, derived from our local sample of AGNs and assuming $S_{24} = 1$ mJy (left) and $S_{70} = 1$ mJy. Each track corresponds to a different AGN from our local sample. Dashed lines correspond to those AGNs whose infrared emission is dominated by star-formation activity, whereas solid lines represent those classed as having AGN-dominated infrared SEDs. For all redshifts considered, 70 μm flux densities provide a significantly more precise measure of the total AGN infrared luminosity, displaying a smaller spread among all tracks.

to further enhance our understanding of AGNs and their role in galaxy evolution.

MIR/FIR AGN DIAGNOSTICS

We use a sample of 36 local (i.e., $z < 0.1$) AGNs to (1) quantify the $L_{\rm IR}/S_{24}$ and $L_{\rm IR}/S_{70}$ ratios as a function of redshift and (2) explore how the S_{70}/S_{24} flux ratio correlates with the relative AGN contribution to the infrared output. To construct this sample, we selected all AGNs from the *Swift*-BAT catalogue that have well sampled 5 - 100 μm (observed) infrared SEDs, incorporating both archival *Spitzer*-IRS spectra and *IRAS* flux densities. By selecting from the *Swift*-BAT catalogue, we ensure that the X-ray properties of this local sample are representative of our main, high redshift sample of AGNs (i.e. $L_{\rm X} \sim 10^{41} - 10^{45}$ ergs^{-1}, $N_{\rm H} > 10^{20}$ cm^{-2} ;[2, 3]). Using the 6.2 um PAH emission feature as an indicator of star formation activity [4], we identify those AGNs whose infrared output is dominated by starbursts. The remainder are classified as AGN-dominated systems.

In Fig. 1 we present the $L_{\rm IR}/S_{24}$ and $L_{\rm IR}/S_{70}$ ratios derived from our sample of local, X-ray detected AGNs. Each track in these plots is derived from an individual AGN's infrared SED, classified in terms of their dominant source of infrared emission (i.e., AGN or starburst). At all redshifts considered, a given S_{70} flux density (in this case, 1 mJy) corresponds to a significantly smaller range in $L_{\rm IR}$ than could be derived from S_{24} alone. For example, estimates of $L_{\rm IR}$ for a $z = 1.5$ source based solely on S_{24} can span over an order of magnitude (i.e., a factor of ~ 12). On the other hand, an equivalent source measured solely at 70 μm would have its $L_{\rm IR}$ constrained to within a factor of ~ 4. We note these quoted ranges of $L_{\rm IR}$ are derived from our full sample of low redshift

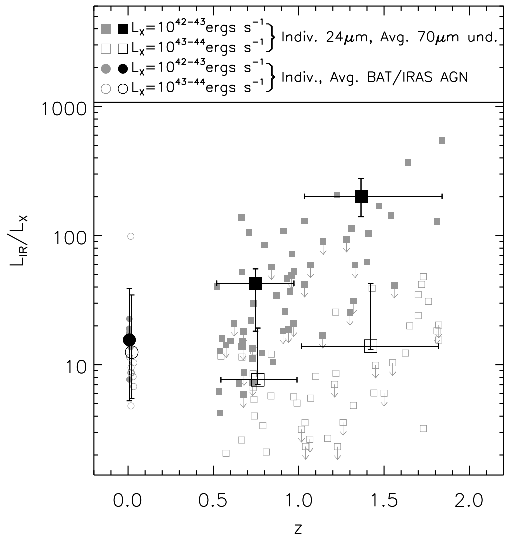

FIGURE 2. $L_{\rm IR}/L_X$ versus redshift for the X-ray detected AGNs in our high and low redshift samples (circles and squares, respectively). Points are filled according to X-ray luminosity (see key). Vertical error bars indicate the range of $L_{\rm IR}/L_X$ produced by assuming the various tracks in Fig. 1. Large, black symbols indicate the results derived from stacking analysis of the 70 μm observations while small, grey squares refer to results derived from individual 24 μm flux densities (upper limits assume a 24 μm limiting sensitivity of 50 μJy; see Mullaney et al. [1] for details). Both the stacking analysis and the individual 24 μm detections clearly show a consistent increase in the $L_{\rm IR}/L_X$ ratio of $L_{\rm X} = 10^{42-43}$ ergs^{-1} AGN from $z \approx 0$ to $z = 1-2$. From Mullaney et al. [1].

AGNs, irrespective of infrared classification (i.e., AGN or starburst-dominated).

By classifying the local X-ray detected AGNs in terms of their dominant source of infrared emission, we can investigate whether the S_{70}/S_{24} flux ratio can be used to identify AGN-dominated systems. This seems plausible based on evidence that, compared to inactive galaxies, AGNs show an excess of MIR emission produced by dust heated by the intense radiation field of the central engine [5]. By exploiting the well constrained SEDs of our local AGN sample, we find that this excess results in AGN-dominated systems having lower S_{70}/S_{24} ratios compared to their starburst-dominated counterparts, with an AGN/starburst division around $S_{70}/S_{24} \sim 5$. This diagnostic remains valid for sources at redshifts < 1.5, beyond which longer wavelength data can be used to discriminate between AGN and starburst-dominated systems (see §4.3 and Fig. 8 of Mullaney et al. 1).

THE MIR-FIR PROPERTIES OF X-RAY AGNS

By applying the above MIR/FIR diagnostics to the high redshift, X-ray detected AGNs in the 1 Ms Chandra Deep Field South (hereafter, CDF-S), we explore how the infrared properties of X-ray detected AGNs vary as a function of redshift and intrinsic power (i.e., $L_{\rm X}$). The intrinsic X-ray luminosities and absorbing column densities of the CDF-S AGNs were taken from Tozzi et al. [6]. The observed 24 μm and 70 μm flux densities of the CDF-S AGNs were obtained from the FIDEL and GOODS *Spitzer* legacy surveys.

However, as only $\sim$10% of the X-ray AGNs in this field are formally detected at 70 μm, we relied on stacking analysis to gain insight into their average infrared properties.

The Strongly Evolving Infrared Luminosities of AGNs

In Fig. 2 we plot the $L_{\rm IR}/L_{\rm X}$ luminosity ratios of the X-ray AGNs as a function of redshift and separated in terms of $L_{\rm X}$. We include in this plot results derived from both our local (i.e., *Swift*-BAT) and high redshift (i.e., CDF-S) samples of X-ray detected AGNs. It is clear from this plot that high redshift, moderate X-ray luminosity AGNs (i.e., defined here as $L_{\rm X} = 10^{42} - 10^{43}$ ergs^{-1}) are significantly more *infrared* luminous (per unit accretion power output) than their low redshift counterparts. Indeed, we note a factor of $12.7^{+7.1}_{-2.6}$ increase in the $L_{\rm IR}/L_{\rm X}$ luminosity ratios between moderate $L_{\rm X}$ AGNs at $z \sim 0$ and $z = 1-2$. However, in the same redshift interval we measure no significant change in the $L_{\rm IR}/L_{\rm X}$ luminosity ratios of the most X-ray luminous AGNs in our sample (i.e., with $L_{\rm X} = 10^{43} - 10^{44}$ ergs^{-1}).

Clearly, results based solely on stacking analysis can be subject to significant systematic uncertainties, not least from the possibility that stacked fluxes can be dominated by a small number of bright sources lying just below the detection threshold of the survey. To check whether such bright, yet undetected, sources are responsible for the observed increase in the $L_{\rm IR}/L_{\rm X}$ luminosity ratios, we also present in Fig. 2 points derived from the 24 μm flux densities of the individual X-ray AGNs. Although measures of $L_{\rm IR}$ derived from S_{24} alone are subject to significant systematic uncertainties (as outlines above), as over 70% of the CDF-S AGNs are detected in at 24 um, such estimates provide an alternative and independent approach to confirming trends derived from the 70 μm stacks. We note that those moderate X-ray luminosity AGNs individually detected at 24 um same follow the trend of increasing $L_{\rm IR}/L_{\rm X}$ luminosity ratio with redshift and are not dominated by small numbers of bright, individual sources.

In summary, both 24 μm and 70 μm data reveal a strongly evolving $L_{\rm IR}/L_{\rm X}$ luminosity ratio among moderate luminosity X-ray AGNs, but there is no evidence of any change among the most luminous X-ray AGNs in our sample.

What is Driving the Observed Increase in $L_{\rm IR}$?

The evolution in $L_{\rm IR}/L_{\rm X}$ for the moderate luminosity AGNs could be due to changes in the AGN dusty torus or increased star-formation in the host galaxies. However, as so few of the CDF-S X-ray AGNs are detected at 70 μm, and the stacked S_{70}/S_{24} ratios lie around the division between AGN and starburst-dominated systems (i.e., $S_{70}/S_{24} \sim 5$), we cannot currently use this diagnostics to distinguish between these scenarios. Because all other major discriminators between AGN activity and star formation (e.g., from *Spitzer*-IRAC photometry; Stern et al. 7) also provide inconclusive results for the dominant source of infrared emission in these AGNs, we consider the impact that *each* of these scenarios would have on our understanding of AGNs and the influence they have on their host galaxies.

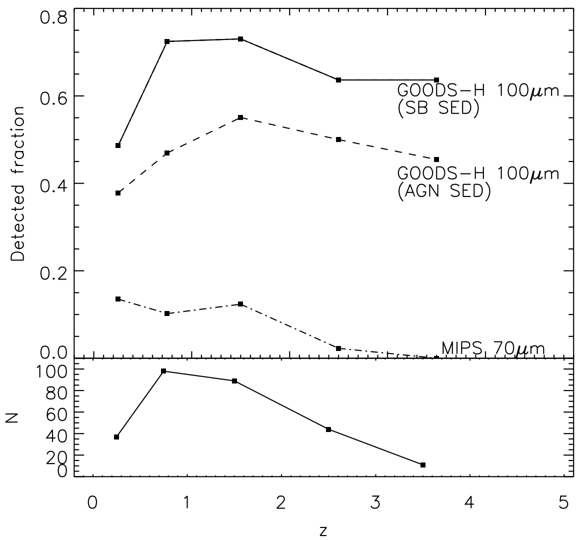

FIGURE 3. *Top:* Predicted fractions of CDF-S X-ray AGNs detected in the upcoming GOODS-H ultra-deep infrared survey to be undertaken by the *Herschel Telescope*. The expected observed 100 μm flux densities are based on 24 μm flux densities of the CDF-S AGNs extrapolated along the average starburst-dominated and AGN-dominated SEDs, derived from our local sample of AGNs. If all the X-ray AGNs were to have starburst-dominated IR SEDs, we would expect to detect *at least* as high a fraction at 100 μm as we currently detect at 24 μm. For comparison we include the fractions of AGNs currently detected at 70 μm. *Bottom:* The total number of CDF-S X-ray AGNs in each bin. From Mullaney et al. [1].

If attributed to star-formation alone, the observed increase in the $L_{\rm IR}/L_{\rm X}$ luminosity ratio would imply a significantly enhanced ratio of galaxy to black hole growth in the early Universe. If all this star-formation were to take place within the bulge of the host galaxy, then this would have a significant impact on the development of black-hole/bulge relationships observed in the local Universe. Using star formation rates derived from Kennicutt [8], we estimate that the ratio between star-formation and mass accretion ($\dot{M}_{\rm SF}/\dot{M}_{\rm Acc} \sim 500$) is comparable to today's BH-bulge mass ratios ($M_{\rm Bulge}/M_{\rm BH} \sim 800$). This could be interpreted as tentative evidence that the links between SMBHs and their host bulges were initially forged at these early times. We note, however, that we have not factored in the growth of inactive galaxies in this assessment.

On the other hand, the increase in the $L_{\rm IR}/L_{\rm X}$ luminosity ratio could also be driven by changes associated with the AGN itself. As the increase is observed in an X-ray luminosity matched sample of AGNs, this change is unlikely to be caused by differences in the power output of the central engine. On the other hand, an increase in the dust covering factor at high redshifts would manifest itself as an increase in the average infrared luminosity. This interpretation agrees, in principle, with results derived from deep X-ray observations that suggest that AGNs in the early Universe were, on average, more heavily obscured than present- a result also supported by evolutionary models of AGNs (e.g. Hasinger 9, Hopkins et al. 10). However, the increase in dust covering factor needed to account for the observed increase in $L_{\rm IR}$ is significantly higher than suggested by those studies. Indeed, if one assumes a typical dust covering factor of $\sim 40\%$ in the local Universe, then a simplistic interpretation of our results would indicate dust

covering factors well in excess of 100% in the early Universe. We note however, that this assumes a linear relationship between L_{IR} and dust covering factor when it is far from clear that this is indeed the case.

Finally, as the measured infrared luminosities of the high-z X-ray AGNs are based solely on extrapolation using the SEDs of local AGNs, it is plausible that the apparent increase in L_{IR} is a result of systematic changes in the SEDs of AGNs across the redshifts considered. Indeed, it has been suggested that the SEDs of purely star-forming galaxies have undergone some degree of change since $z \sim 2$ (e.g., Magnelli et al., *in prep.*). Perhaps this could be also true for AGNs? However, with so few high redshift X-ray AGNs detected at far-infrared wavelengths, it is extremely difficult to determine whether this is indeed the case. Future deep surveys to be undertaken by *Herschel* promise to remedy this situation and distinguish between these different scenarios.

Irrespective of the cause of the increased infrared luminosity, a thorough understanding of how L_{IR}/L_X evolves will be necessary in order to identify potential X-ray weak, infrared bright AGNs at high redshifts and determine their intrinsic luminosities.

PREDICTIONS FOR DEEP HERSCHEL OBSERVATIONS

With its vastly superior sensitivity at far-infrared wavelengths, the recently launched *Herschel Observatory* will probe a whole new region of the $L_{IR} - z$ parameter space. Our estimates (based on extrapolation of the 24 μm flux densities) indicate that as many as 70% of the X-ray detected AGNs in the CDF-S will be detected at 100 μm in the planned ultra-deep *Herschel* observations of this field (i.e., GOODS-H, P.I.: D. Elbaz; see Fig. 3), compared to the ~10% detected in the deepest *Spitzer* FIR surveys. With such large numbers of detections, we will be able to constrain the far-infrared SEDs of the majority of the X-ray AGNs in the deep fields, providing clear insights into the dominant source of infrared emission in these objects (i.e., AGN or star-formation activity). This, in turn, will enable us to establish the full extent and cause of the observed increase in the L_{IR}/L_X luminosity ratio. Furthermore, the diagnostics described here and in Mullaney et al. [1] provide the means to use *Herschel* photometry to identify significant numbers of AGN-dominated systems, including those X-ray weak, Compton-thick AGNs currently missed at all other wavelengths.

REFERENCES

1. J. R. Mullaney et al., *MNRAS* **401**, 995–1012 (2010).
2. D. M. Alexander et al., *AJ* **126**, 539–574 (2003).
3. L. M. Winter , R. F. Mushotzky, C. S. Reynolds, and J. Tueller, *ApJ* **690**, 1322–1349 (2009).
4. R. Genzel et al., *ApJ* **498**, 579–+ (1998).
5. M. H. K. de Grijp, J. Lub, and G. K. Miley, *A&ASS* **70**, 95–114 (1987).
6. P. Tozzi et al., *A&A* **451**, 457–474 (2006).
7. D. Stern et al., *ApJ* **631**, 163–168 (2005).
8. R. C. Kennicutt, Jr., *ARA&A* **36**, 189–232 (1998).
9. G. Hasinger, *A&A* **490**, 905–922 (2008).
10. P. F. Hopkins et al., *ApJS* **163**, 1–49 (2006).